

Multiscale fMRI analysis reveals hierarchical network disruptions underlying disorders of consciousness

S.A. Kurkin^{ID}*,¹, L.A. Mayorova^{ID}¹, V.S. Khorev^{ID}, E.N. Pitsik^{ID}, M.L. Radutnaya^{ID},
E.L. Bondar^{ID}, A.E. Hramov^{ID}

Federal Research and Clinical Center of Intensive Care Medicine and Rehabilitation, Lytkino, 777, Solnechnogorsk, 141534, Russia

ARTICLE INFO

Keywords:

Disorders of consciousness
Anoxic brain injury
Vegetative state
Minimally conscious state
fMRI
Functional brain networks
Large-scale networks
Multiscale analysis
Multigraph model

ABSTRACT

Disorders of consciousness following anoxic brain injury present profound clinical and scientific challenges, with current diagnostic methods often failing to capture underlying neuronal network pathophysiology. Here, we develop a novel multiscale framework combining global, macro-, and local-level network analyses to characterize functional connectivity alterations in vegetative (VS) and minimally conscious states (MCS) in patients with anoxic brain damage/ after anoxic brain damage. While global network architecture remained preserved, macro-level analyses revealed selective disruptions in the cingulate operculum and ventral attention networks, with opposing centrality patterns suggesting network-specific reorganization. Modified participation coefficients demonstrated widespread imbalances in integration-segregation across large-scale networks, particularly affecting perception and salience systems. Network-based statistics identified a conserved triangular hypo-connectivity pattern (anterior cingulate-orbitofrontal-temporal) alongside state-specific hyperconnectivity profiles in VS and MCS patients compared to healthy controls. Our multigraph integration revealed asymmetric reorganization: VS patients exhibited extensive compensatory hyperconnectivity, while MCS showed predominant hypo-connectivity with partial VAN-mediated compensation. These findings establish a hierarchical model of consciousness impairment, where core network disruptions interact with state-dependent compensatory mechanisms. The multiscale approach provides clinically actionable biomarkers while advancing theoretical understanding of neural correlates of consciousness, offering new avenues for targeted interventions.

1. Introduction

The development of objective neuroimaging-based diagnostic tools represents a crucial advancement for intensive care units managing patients with disorders of consciousness (DoC). Contemporary neuroscience conceptualizes consciousness as an emergent property of integrated brain network function [1–3], positioning advanced functional magnetic resonance imaging (fMRI) and diffusion tensor imaging (DTI) as particularly promising modalities for characterizing these complex conditions [4]. Traditional fMRI studies have focused on demonstrating preserved cortical responses to speech, visual stimuli, and cognitive tasks in minimally conscious state (MCS) patients, unlike vegetative state (VS) patients. However, there remains an urgent need for reliable biomarkers that can objectively differentiate clinical states, including chronic DoC, and predict recovery trajectories.

* Corresponding author.

E-mail addresses: kurkinsa@gmail.com (S.A. Kurkin), larimayor@gmail.com (L.A. Mayorova), khorevvs@gmail.com (V.S. Khorev), pitsikelena@gmail.com (E.N. Pitsik), doctor.radutnaya@gmail.com (M.L. Radutnaya), bondar@fncrr.ru (E.L. Bondar), hramovae@gmail.com (A.E. Hramov).

¹ These authors contributed equally to this work.

<https://doi.org/10.1016/j.chaos.2025.117008>

Received 3 June 2025; Received in revised form 29 July 2025; Accepted 4 August 2025

Available online 14 August 2025

0960-0779/© 2025 Elsevier Ltd. All rights are reserved, including those for text and data mining, AI training, and similar technologies.

Table 1
Demographic and clinical data of the patients included in this study.

Patient id	Diagnosis	Age	Sex	CRS-R	FOUR
1	VS	39	F	6	13
2	VS	49	F	5	6
3	VS	40	F	6	9
4	VS	32	M	4	7
5	VS	62	F	3	12
6	VS	44	F	1	3
7	VS	30	M	5	6
8	VS	51	M	3	9
9	VS	32	M	5	13
10	VS	39	M	5	11
11	VS	32	M	5	10
12	VS	22	F	6	9
13	VS	35	M	12	14
14	VS	34	F	4	9
15	VS	47	F	5	10
16	VS	58	M	6	10
17	VS	43	F	2	8
18	VS	39	F	9	13
19	MCS	40	M	7	9
20	MCS	47	M	11	13
21	MCS	37	M	8	14
22	MCS	32	M	9	10
23	MCS	64	M	11	13
24	MCS	39	F	12	13
25	MCS	39	F	10	15

Recent paradigm shifts in consciousness research emphasize the importance of intrinsic functional network organization rather than isolated regional responses [5–7]. This systems-level perspective builds on evidence that consciousness depends on the dynamic integration of large-scale brain networks (LSNs), particularly those involved in sensory processing, attention, and self-referential cognition [1,8]. The hierarchical organization of these networks along unimodal-transmodal gradients appears critical for maintaining conscious awareness [1], with disruptions to this architecture leading to characteristic impairments in DoC [4]. However, current network approaches often fail to capture the multiscale nature of consciousness-related network disruption, where global architecture may remain intact while critical subsystem interactions become impaired [3,9].

We hypothesize that chronic DoC arise from specific disruptions in LSN interactions that manifest across multiple spatial scales. This aligns with emerging frameworks that view consciousness impairment as a disturbance in the brain's capacity to integrate information while maintaining functional diversity [2,4]. To test this, we developed a novel multiscale analytical framework that: (1) examines network organization at global, macro, and local levels, (2) introduces a modified participation coefficient that quantifies imbalances in network integration and segregation, and (3) integrates these findings through multigraph model to visualize how focal disruptions affect the entire system. This approach bridges an important gap between local-scale connectivity changes and their system-wide functional consequences.

Our work advances the field in three key dimensions. First, the methodological innovation of combining quantitative multiscale network metrics with qualitative multigraph modeling provides a new paradigm for studying complex neurological disorders. Second, the identification of specific network biomarkers of anoxic DoC offers clinically actionable targets for diagnosis and monitoring. Third, these findings contribute fundamental insights into the neural architecture of consciousness, revealing how hierarchical network disruption gives rise to different impairment states. By elucidating the network mechanisms underlying DoCs, this research moves us closer to precision medicine approaches for these challenging conditions.

2. Materials and methods

2.1. Subjects

The study involved 12 healthy control subjects (HC group, 8 female, age 42.1 ± 5.4) and 25 patients with anoxic (or toxic) brain injury in a vegetative state (VS group, 17 patients, 10 female, age 40.4 ± 7.8) or minimally conscious state (MCS group, 8 patients, 3 female, age 42.2 ± 7.4). All patients were admitted to the Federal Research and Clinical Center for Intensive Care Medicine and Rehabilitology (Moscow, Russia) between 2022 and 2025. Clinical assessment of consciousness was performed using the FOUR (Full Outline of UnResponsiveness) score [10] and CRS-R (Coma Recovery Scale - Revised) score [11]. The lowest item on each subscale represents reflexive activity, while the highest item represents cognitively mediated behaviors by addressing to auditory, visual, motor, oromotor, communication, and arousal functions. More detailed information on demographic and clinical data of the patients is presented in Table 1. The groups show statistically significant difference in diagnostic scores but not in age (Mann–Whitney nonparametric test, u - and p -values are presented in Table 2).

Table 2

Statistical differences between groups in age and diagnosis scores (CRS-R and FOUR).

Groups\Measure	u-value Age	p-value	u-value CRS-R	p-value	u-value FOUR	p-value
HC vs. VS	0.0212	0.9831	–	–	–	–
HC vs. MCS	–0.0847	0.9325	–	–	–	–
VS vs. MCS	–0.3654	0.7148	–3.2696	0.001	–2.2074	0.027

The study adhered to the ethical principles established in the 1964 Helsinki Declaration and its subsequent revisions, with approval from the local Bioethical Committee of the Federal Research and Clinical Center for Intensive Care Medicine and Rehabilitology (Moscow, Russia). All healthy participants and patients' relatives provided voluntary written informed consent, allowing for the publication of any potentially identifiable images or data included in this manuscript.

2.2. Data acquisition

Resting-state functional magnetic resonance imaging (fMRI) data were acquired using a 1.5 T Siemens Essenza scanner (Siemens, Ltd., Germany) equipped with an eight-channel head coil. Resting-state functional images were collected in 300 T2-weighted echoplanar imaging (EPI) volumes per run, with an in-plane resolution of $3.9 \text{ mm} \times 3.9 \text{ mm}$, 4.0-mm slice thickness, and 0.8-mm interslice gap. The EPI sequence had a repetition time (TR) of 3670 ms, an echo time (TE) of 70 ms, and a matrix size of 64×64 . A high-resolution T1-weighted anatomical scan was also acquired for each participant, consisting of 192 slices with a voxel size of $1 \text{ mm} \times 1 \text{ mm} \times 1 \text{ mm}$, a TR of 10 s, a TE of 4.76 ms, and an acquisition matrix of 256×256 .

2.3. Preprocessing and reconstruction of brain functional network

The whole pipeline of the study is schematically represented in Fig. 1. The SPM statistical processing package [12] was utilized for data processing in MATLAB (version 2019b). Standard preprocessing procedures were employed to the fMRI data (Fig. 1, panel I), including motion correction, co-registration with the high-resolution T1 image, and normalization to the Montreal Neurological Institute (MNI) standard space [13–15].

Employing the AAL3 anatomical atlas [16], we parcellated the brain into 165 distinct areas. Then, the functional connectivity between all pairs of these areas was quantified with a connectivity matrix (Fig. 1, panel II). We obtained this matrix by averaging the BOLD time series within each of the 165 regions, treating each as a network node. Following detrending of these averaged time series, pairwise Pearson correlation coefficients were calculated across all nodes. This connectivity matrix effectively represents the functional brain network, illustrating the strength of coupling between different brain regions based on their BOLD signal correlations [17]. We then performed a p-value-based thresholding of the functional brain networks: we keep only significant connections that have a p-value in the Pearson correlation of less than 0.05 [18]. For the calculation of network measures, the values in the matrices were taken modulo.

2.4. Levels of network analysis

Our approach analyzes network interactions at three distinct levels:

- Global level: Interactions between subnetworks—large-scale networks (LSNs)—treated as single units or macronodes [19,20].
- Macro level: Interactions between subnetworks, accounting for both (i) intra-subnetwork node interactions and (ii) inter-subnetwork node connections [21,22].
- Local level: Interactions between individual nodes within the original network.

We analyzed 12 subnetworks (see Table 3) from [23], encompassing all major LSNs. The global correlation matrix (12×12) was constructed using pairwise Pearson correlations between subnetworks, derived from their mean BOLD signals (averaged across constituent nodes — see Fig. 1, panels II and III).

At the macro level, correlation matrices captured node-wise interactions within and between subnetworks.

2.5. Network characteristics

2.5.1. Network measures

A number of network characteristics were calculated at the global level — for the network of subnetworks — as well as at the macro level — for each of the subnetworks. Specifically, the following measures were used [24].

- Clustering Coefficient: Quantifies local network cohesiveness by measuring the tendency of nodes to form tightly connected clusters. It reflects the density of connections among a node's direct neighbors [25].
- Node Strength: The sum of connection weights attached to a node, indicating its total interaction magnitude within the network [26].

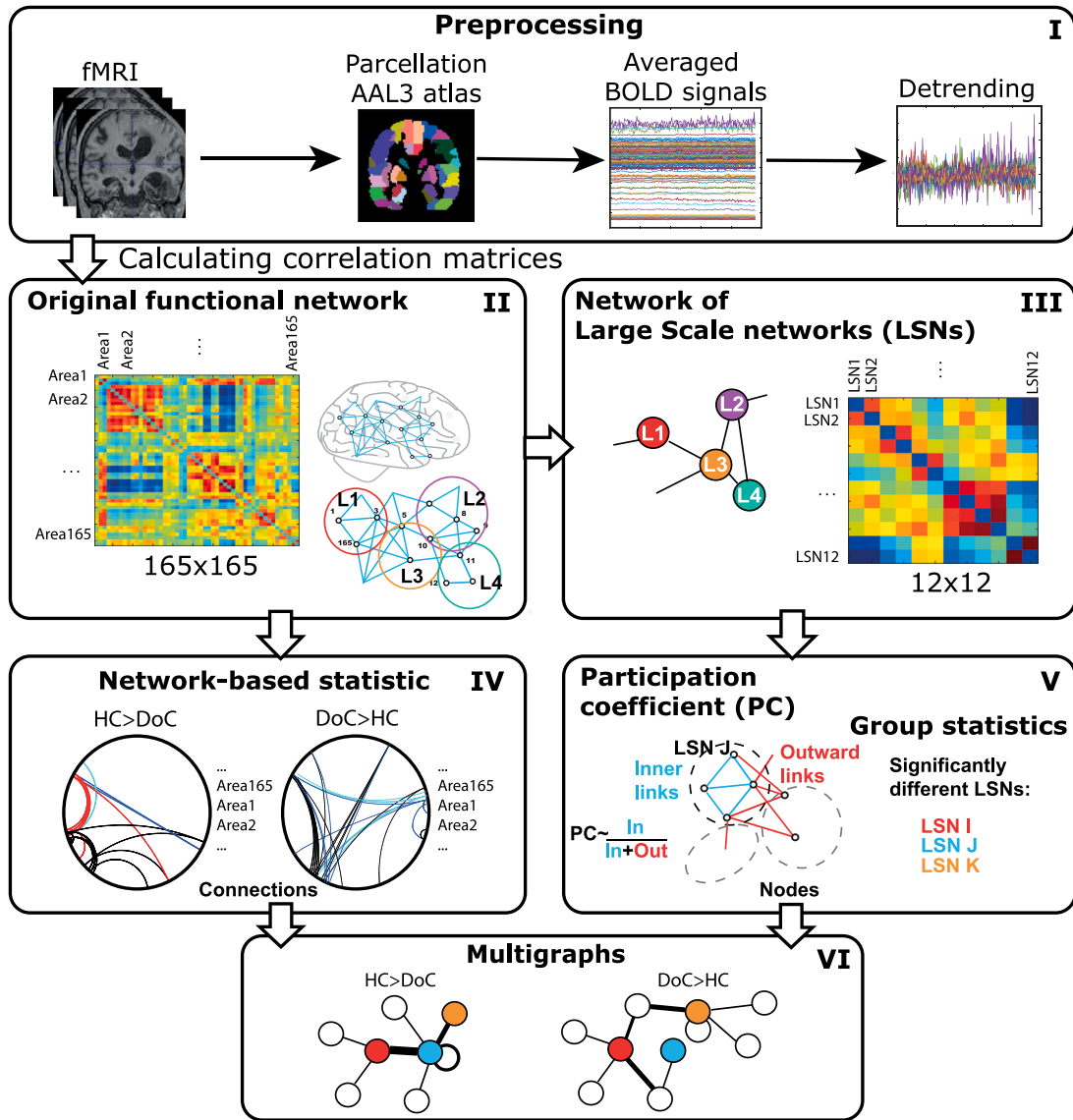


Fig. 1. Flowchart of the research.

- **Global Efficiency:** Represents the network's capacity for efficient information transfer, calculated as the average inverse shortest path length between all node pairs. Higher values indicate greater integrative capacity [27].
- **Eigenvector Centrality:** Measures a node's influence based on its connections to other highly central nodes. Computed from the dominant eigenvector of the adjacency matrix, it identifies key nodes in the network's structural hierarchy [28].

Network measures were averaged over the corresponding nodes.

2.5.2. Modified participation coefficient

We employed a modified participation coefficient (PC) adapted for the case of a single network community (Fig. 1, panel V):

$$P_i = 1 - \left(\frac{w_{is}}{w_i} \right)^2, \quad (1)$$

where P_i represents the modified PC for node i , w_{is} denotes the total connection weight between node i and other nodes within its community, and w_i is the node's total strength (sum of all connection weights, both within and outside the community). This modified PC quantifies how peripheral a node is to its community, where values approaching 1 indicate connector nodes with predominantly external connections (gateway nodes), while values near 0 correspond to core nodes with primarily internal connections.

Table 3

Considered large-scale networks (LSNs)/subnetworks.

Source: From [23].

LSN	Abbreviation	Constituent brain regions (nodes)
Cingulate Operculum	COper	Anterior insula/Operculum, Dorsal anterior cingulate cortex, Thalamus
Context network	Context	Parahippocampal cortex, Retrosplenial cortex
Default Mode Network	DMN	Posterior cingulate cortex, Precuneus, Medial prefrontal cortex, Angular Gyrus
Dorsal Attention Network	DAN	Visual motion area, Frontal eye fields, Superior Parietal Lobule Intraparietal Sulcus, Ventral premotor cortex
Perception Network	perN	Lateral Orbitofrontal, Ventromedial temporal, Temporal pole, Subgenual Anterior cingulate cortices, Fusiform Gyrus, Rostral superior Temporal sulcus, Ventrolateral Amygdala
Somatomotor Network	Somatomotor	S1, M1, Supplementary Motor Area (SMA), Thalamus
Striatum	Striatum	Caudate, Putamen, Ventral Striatum
Thalamus	Thalamus	Thalamic Nuclei, Subcortical regions
Ventral Attention Network	VAN	Bilateral Ventrolateral prefrontal cortex, Bilateral temporal–parietal junction
Visual network	Visual	Middle temporal visual association area at the temporal–occipital junction
Fronto-parietal Network	FPN	Intraparietal Sulcus, Ventral Inferior Temporal Lobe, Lateral prefrontal cortex
Saliience Network	SN	Limbic and Prefrontal regions, Amygdala, Anterior Insula, Dorsal anterior cingulate cortex, Ventral striatum

To characterize whole communities, we computed the community-averaged PC:

$$\langle P \rangle_k = \frac{1}{|C_k|} \sum_{i \in C_k} P_i, \quad (2)$$

where C_k represents the set of nodes in community k and $|C_k|$ is the community size. The averaged PC provides insights into community organization: low values ($\langle P \rangle \rightarrow 0$) indicate strongly segregated communities with predominantly internal connections, while high values ($\langle P \rangle \rightarrow 1$) suggest communities heavily dependent on external connections. A balanced community with equal internal and external connectivity would yield $\langle P \rangle = 0.75$.

In our macro level analysis, we treated the 12 predefined LSNs as distinct communities ($k = 1, \dots, 12$) and computed their averaged PCs separately. This modified approach addresses two critical limitations of the standard PC formulation [29]: (1) it eliminates ambiguity in defining PC for nodes shared between communities (common in LSNs), and (2) it provides a robust characterization of a community's integrative (external connectivity) and segregative (internal connectivity) properties.

In the following, we will refer to the modified version of the PC as simply the participation coefficient or PC.

2.6. Statistical analysis

For local network-level comparisons, we applied the network-based statistic (NBS) method [30] to identify significantly altered subnetworks in the complete 165×165 connectivity matrix between groups (Fig. 1, panel IV). The analysis was performed with 50,000 permutations using a primary threshold of $t = 3.5$ ($p = 0.05$), providing robust control for multiple comparisons while maintaining sensitivity to detect connected patterns of altered connectivity.

At the global and macro levels, we compared network measures between groups using the Mann–Whitney U test. This nonparametric approach was chosen because it makes no assumptions about data normality and is robust to outliers. The test was applied to node-averaged values of each network metric to evaluate systematic between-group differences in network topology.

To account for multiple comparisons across subnetworks and network measures, we implemented Bonferroni correction. We applied the correction separately for each class of network measures (e.g., node strength, clustering coefficient) across all 12 subnetworks, ensuring rigorous control of false positives while maintaining interpretability of results.

2.7. Multigraph representation of disrupted network interactions

We developed a multigraph model to visualize disrupted interactions between LSNs associated with consciousness disorders (Fig. 1, panel VI). The model was constructed by first defining macronodes as those LSNs that showed significant between-group differences in participation coefficient values, highlighting networks with altered integration–segregation balance. We then incorporated significant between-group connections identified through NBS analysis of the complete 165×165 connectivity matrix, which included both inter-LSN connections (between the defined macronodes) and any additional connected LSNs needed to preserve network context. Intra-LSN disruptions within the defined macronodes were represented as self-referential loops to capture local network disturbances.

In this representation, edge thickness corresponds to the number of disrupted connections between LSN pairs, providing a quantitative visualization of connection alterations. The multigraph integrates information across scales by combining macroscale

Table 4

Between-group comparisons of global-level network measures. Statistical tests were performed for the network of large-scale networks (LSNs), with no significant differences observed; comparisons shown for healthy controls (HC), vegetative state (VS), and minimally conscious state (MCS) groups.

Measure	u-value HC > VS	p-value	u-value HC > MCS	p-value	u-value MCS > VS	p-value
Global efficiency	−0.3321	0.7398	−0.5015	0.6160	0.2039	0.8384
Eigenvector centrality	0.2879	0.7735	0.4243	0.6713	0.0001	0.9999
Node strength	−0.5093	0.6105	0.1929	0.8471	−0.4953	0.6204
Clustering coefficient	−0.4650	0.6419	0.2700	0.7871	−0.4953	0.6204

Table 5

Between-group differences in eigenvector centrality at the macro level across predefined large-scale networks (LSNs) without Bonferroni correction. Comparisons shown for healthy controls (HC), vegetative state (VS), and minimally conscious state (MCS) groups.

LSN	u-value HC > VS	p-value	u-value HC > MCS	p-value	u-value MCS > VS	p-value
COper	1,794	0,073	2,276	0,023*	−0,612	0,541
Context	−0,864	0,388	−1,119	0,263	0,437	0,662
DMN	−1,395	0,163	−1,659	0,097	0,845	0,398
DAN	−1,174	0,241	−1,196	0,232	0,087	0,930
perN	0,376	0,707	0,964	0,335	−0,728	0,466
Somatomotor	1,749	0,080	1,890	0,059	−0,204	0,838
Striatum	1,041	0,298	0,887	0,375	−0,087	0,930
Thalamus	1,174	0,241	1,890	0,059	−0,554	0,580
VAN	−2,148	0,032*	−2,199	0,028*	0,728	0,466
Visual	1,351	0,177	1,504	0,132	−1,020	0,308
FPN	−1,749	0,080	−1,119	0,263	−0,379	0,705
SN	−1,085	0,278	−0,887	0,375	0,000	1,000

* Significant effects.

PC changes (through node selection criteria) with mesoscale connectivity disruptions (through edge topology) and local network disturbances (through self-loops). This approach effectively captures how localized connection changes propagate to produce LSN-level alterations in integration–segregation balance, and how these changes manifest in the overall network organization. The resulting model provides a comprehensive framework for understanding the hierarchical nature of network disruptions in consciousness disorders, linking local connectivity changes to global network reorganization through identifiable intermediate LSN-level effects.

The multigraph representation offers several advantages for analyzing network disruptions in clinical populations. First, it maintains the quantitative nature of the underlying connectivity data while providing an intuitive visualization. Second, it reveals patterns of network disturbance that might be obscured when examining individual connections or network metrics in isolation. Finally, by combining results from complementary analysis approaches (PC and NBS), it provides a more complete picture of network dysfunction than either method could offer alone. This integrated visualization approach helps identify potential network hubs and pathways that may be particularly vulnerable in consciousness disorders, suggesting targets for further investigation and potential therapeutic intervention.

3. Results

Global-level analysis of the network organization revealed no significant differences in network measures between groups (Table 4), indicating preserved global architecture for the network of LSNs across all subject groups.

At the macro level, eigenvector centrality showed significant (without Bonferroni correction) between-group differences in specific subnetworks. The cingulate operculum network demonstrated significant differences between healthy control (HC) group and minimally conscious state (MCS) patients and near-significant alterations between HC and vegetative state (VS) patients ($p = 0.07$), while the ventral attention network (VAN) exhibited significant differences in both HC-VS and HC-MCS comparisons (Table 5, Appendix). Notably, eigenvector centrality values were higher in healthy controls for the cingulate operculum network but lower in the VAN compared to patient groups (Fig. 2). No significant differences emerged between patient groups (VS vs. MCS). No significant effects were found for clustering coefficient and node strength (See Tables 7 and 8, Appendix).

These findings suggest selective alterations in intra-network connectivity patterns, particularly affecting the cingulate operculum and ventral attention networks, while preserving global network organization. The observed changes in eigenvector centrality indicate modified functional influence of key nodes within these specific subnetworks in patients with DoC.

Analysis of subnetwork-averaged participation coefficient (PC) revealed substantial between-group differences in multiple large-scale networks (Table 6). Prior to multiple comparisons correction, we observed significant PC differences between HC group and VS patients in 8 of 12 subnetworks, and between HC and MCS patients in 5 subnetworks. Affected LSNs common to both comparisons included the context, perception, ventral attention, visual, and salience networks, with consistently higher PC values in patient groups relative to controls.

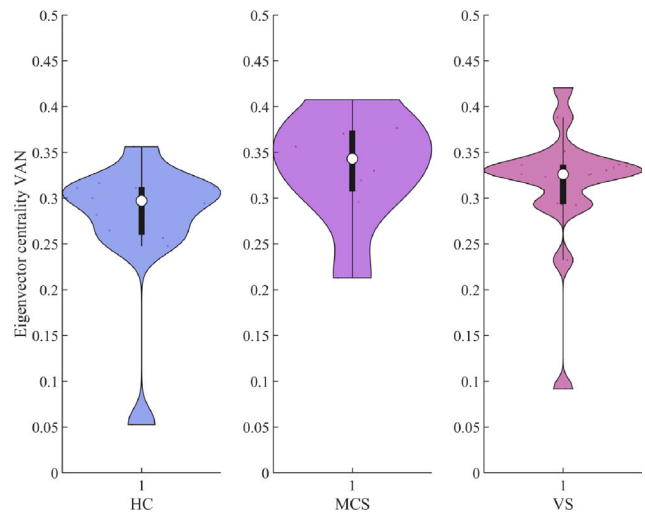


Fig. 2. Eigenvector centrality distributions in the ventral attention network (VAN) with boxplots across study groups (HC = healthy controls, VS = vegetative state, MCS = minimally conscious state).

Table 6
Between-group differences in participation coefficient at the macro level across predefined large-scale networks (LSNs); p_B denotes the Bonferroni-corrected p -value, p_B is not shown for the MCS vs. VS due to lack of significant effects.

LSN	u-value HC < VS	p -value	p_B -value	u-value HC < MCS	p -value	p_B -value	u-value MCS > VS	p -value
COper	0,191	0,849	1,000	0,000	1,000	1,000	−0,361	0,718
Context	3,832	0,000*	0,002**	1,967	0,049*	0,590	−1,528	0,127
DMN	0,910	0,363	1,000	0,193	0,847	1,000	−0,806	0,420
DAN	1,969	0,049*	0,588	0,579	0,563	1,000	−0,028	0,978
perN	3,578	0,000*	0,004**	3,279	0,001*	0,013**	0,306	0,760
Somatomotor	1,969	0,049*	0,588	1,659	0,097	1,000	0,306	0,760
Striatum	1,376	0,169	1,000	0,810	0,418	1,000	−0,139	0,890
Thalamus	1,080	0,280	1,000	1,042	0,298	1,000	0,361	0,718
VAN	2,604	0,009*	0,111	2,893	0,004*	0,046**	0,306	0,760
Visual	2,392	0,017*	0,201	2,199	0,028*	0,335	0,639	0,523
FPN	2,858	0,004*	0,050**	1,582	0,114	1,000	0,000	1,000
SN	2,858	0,004*	0,050**	2,585	0,010*	0,117	0,000	1,000

* Significant effects.
** Bonferroni-corrected.
significant effects.

After applying Bonferroni correction for 12 comparisons, several networks maintained significant between-group differences. The HC-VS comparison showed altered PC in context, perception, fronto-parietal, and salience networks, while the HC-MCS comparison revealed differences in perception and ventral attention networks. Notably, the perception network exhibited consistent PC changes across both patient groups (Fig. 3), suggesting its potential role as a universal marker of consciousness impairment. No significant differences emerged between VS and MCS patient groups.

At the local level, the NBS analysis identified significant alterations in functional connectivity specific to DoC (Fig. 4). A particularly robust finding was the consistent pattern of reduced connectivity in patient groups (both VS and MCS) relative to HC, forming a triangular network involving three key regions: the anterior cingulate cortex (ACC), medial orbitofrontal/rectus regions, and inferior temporal cortex. This conserved hypo-connectivity pattern suggests a fundamental network disruption associated with impaired consciousness.

In contrast, patterns of increased connectivity (VS > HC and MCS > HC) displayed markedly different configurations with minimal overlap between patient groups. This directional specificity reveals that while reduced connectivity patterns are largely conserved across consciousness disorder states, increased connectivity patterns are state-dependent and differ substantially between VS and MCS. The distinct triangular ACC-orbitofrontal-temporal network emerges as a consistent marker of consciousness impairment, whereas hyper-connectivity patterns appear more variable and condition-specific.

These results demonstrate that DoC involve both shared network deficits and state-dependent connectivity alterations. The findings point to a complex reorganization of functional networks that reflects both core impairments common across consciousness disorders and adaptive or maladaptive changes specific to different levels of impairment severity.

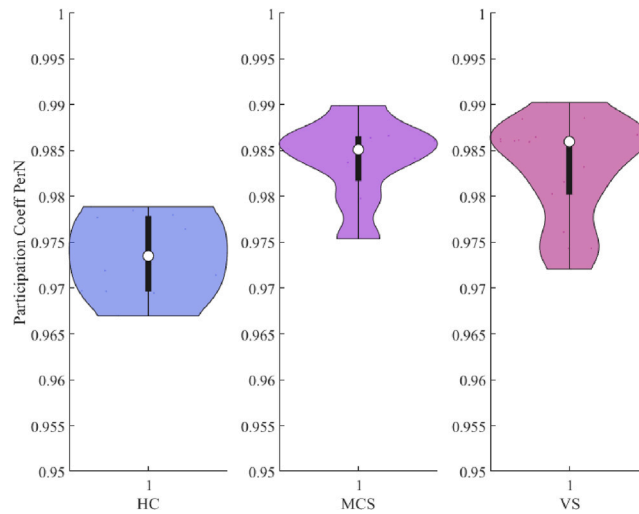


Fig. 3. Participation coefficient distributions in the perception network (perN) with boxplots across study groups (HC = healthy controls, VS = vegetative state, MCS = minimally conscious state).

Using our established multigraph framework (Section 2.7), we constructed comprehensive models integrating both significant differences in large-scale network participation coefficients and altered functional connections between HC and patient groups (Fig. 5). The models revealed several important findings regarding network disruption patterns. A consistent subnetwork involving the ventral attention network (VAN), salience network (SN), perception network (PerN), and striatum appeared in both comparison directions (HC > patients and HC < patients), with the exception of MCS > HC which only involved VAN and SN. This core network configuration suggests these regions play a fundamental role in consciousness disorders.

We observed notable asymmetries in network involvement between patient groups. Vegetative state patients (VS) showed more extensive alterations when compared to controls (8 macronodes in VS > HC versus 4 in HC > VS). The pattern reversed for minimally conscious patients (MCS), where controls showed greater network differences (9 macronodes in HC > MCS versus 5 in MCS > HC). These directional differences in network reorganization imply distinct pathological mechanisms underlying different consciousness impairment states.

The most prominent differences emerged in inter-network connectivity. For VS patients, the strongest hyperactivated connections (VS > HC) involved: (1) salience network (SN) interactions with ventral attention network (VAN), cingulate operculum (COper), context network, and default mode network (DMN) and (2) context-striatum pathways. In MCS patients, we observed distinct patterns: hyperactivated MCS > HC connections involved VAN-COper and VAN-thalamus pathways, while hypoactivated MCS < HC connections included PerN links with striatum, visual network, and SN, plus VAN-SN and VAN-striatum connections. Notably, intra-network alterations appeared exclusively in the PerN (MCS < HC), suggesting specific internal disconnection in this network for MCS patients.

These findings demonstrate two fundamental aspects of consciousness impairment: (i) a consistently affected core network (VAN, SN, PerN, striatum) across all comparisons, and (ii) state-dependent patterns of network disruption that differ between vegetative and minimally conscious states, potentially reflecting different compensatory mechanisms or pathological processes.

Thus, the multigraph models collectively reveal:

- A hierarchical pattern of network disruption, from conserved inter-network alterations to state-specific connectivity changes.
- Potential markers distinguishing VS from MCS based on their characteristic connectivity signatures.
- Differential vulnerability of network subsystems, with perception networks showing particular sensitivity in MCS.

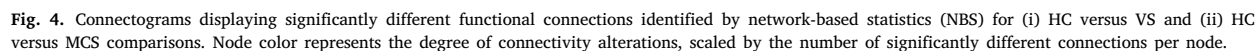
4. Discussion

Our multiscale network analysis revealed distinct patterns of disruption across different degrees of consciousness impairment.

4.1. Global and macro level disruptions in disorders of consciousness

At the global level, the overall architecture of LSNs interaction, characterized by averaged network measures, remained intact across both groups.

However, macro level analysis uncovered selective intra-network alterations in specific subnetworks, particularly showing altered eigenvector centrality in the cingulate operculum and ventral attention networks (VAN). These changes manifested as increased centrality in the HC group for the cingulate operculum but decreased centrality for the VAN compared to the patient groups,



Conversely, the VAN showed the opposite pattern, with elevated centrality in patient groups. This finding may represent either:

- The bidirectional nature of these centrality changes (increased in one network but decreased in another) underscores the complex, network-specific pathophysiology underlying consciousness disorders. The cingulate operculum's reduced influence may impair global integration, while VAN hyper-centrality could lead to unbalanced attentional processing. Together, these alterations may disrupt the normal interplay between bottom-up (VAN-mediated) and top-down (cingulate-mediated) processes necessary for conscious awareness [34].

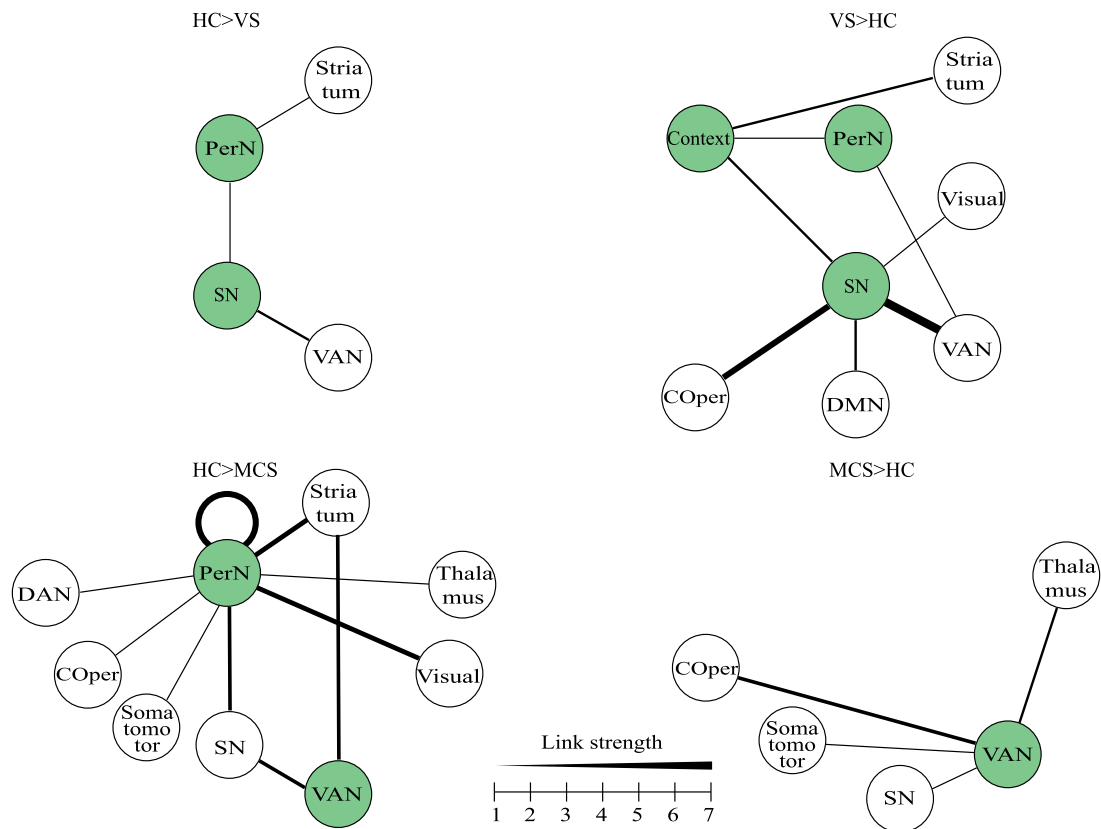


Fig. 5. Multigraph models of network alterations combining: significant differences in large-scale network (LSN) participation coefficients (PCs) and altered functional connections identified by network-based statistics (NBS). Models compare (i) HC versus VS and (ii) HC versus MCS patients. The link strength range corresponds to the number of significant NBS connections. Green macronodes indicate LSNs with significant between-group PC differences. (For interpretation of the references to color in this figure legend, the reader is referred to the web version of this article.)

4.2. Interpretation of participation coefficient alternations

The analysis of PC provides unique insights into network reorganization in DoC by simultaneously capturing both intra-network and inter-network connectivity properties. While calculated at the macro level, PC's special value lies in this dual perspective — it reflects how subnetworks maintain their internal organization while interacting with the broader network architecture (see also Section 2.5.2).

The consistently elevated PC values in patient groups compared to HC reveal a fundamental disruption of the normal integrative-segregative balance in a number of LSNs. Higher PC values indicate a relative shift toward greater inter-network connectivity at the expense of intra-network connections. This pattern suggests two concurrent pathological processes: first, a breakdown of normal within-network communication that may reflect LSN disintegration, and second, a compensatory over-reliance on between-network connections that could represent maladaptive network reorganization. The perception network's particularly consistent alterations across both VS and MCS patients aligns with its known role as a primary gateway for sensory information integration [34], making it especially vulnerable to consciousness disturbances.

The reduced severity of PC alterations in MCS compared to VS patients likely reflects the better state of consciousness function in MCS patients compared to VS patients. The better preserved intra-network connectivity in MCS patients implies that some structural integrity remains, potentially providing a substrate for therapeutic interventions targeting network reintegration.

The VAN findings create a particularly compelling narrative when combined with the centrality results. While the centrality analysis showed the VAN's increased influence within the broader network (suggesting hyperactivation), the PC results reveal this comes at the cost of reduced within-network cohesion. In other words, the increase in the VAN centrality is due to an increase in inter-network connections, while internal connections are disrupted. This paradox mirrors observations in other neurological conditions where networks can become hyperconnected yet functionally inefficient [36]. The VAN's dual disruption may be especially detrimental given its normal role in switching between internal and external awareness [37] — a critical function for conscious experience.

These PC patterns have important theoretical implications. The perception network's vulnerability supports models emphasizing sensory integration in consciousness generation [38], while the VAN's dual disruption aligns with theories prioritizing attentional

mechanisms [39]. The gradient of abnormalities from VS to MCS provides empirical support for the hierarchical models of changes in consciousness [40]. Clinically, the PC's sensitivity to both integration and segregation makes it particularly valuable for tracking recovery and potentially predicting treatment response, as network reintegration often precedes behavioral improvement [41].

4.3. Local network disruptions in disorders of consciousness

Local-level network-based statistics (NBS) identified a conserved triangular network of reduced connectivity in patients involving anterior cingulate, orbitofrontal, and inferior temporal regions, alongside state-dependent patterns of hyperconnectivity that differed between VS and MCS groups.

The network-based statistic (NBS) results reveal a fundamental tripartite network disruption in DoC, centered on three critical regions: the anterior cingulate cortex (ACC), medial orbitofrontal/rectus areas, and inferior temporal cortex. This triangular hypo-connectivity pattern, conserved across both VS and MCS patients, likely represents a core neural signature of impaired consciousness. The ACC's involvement is particularly noteworthy given its well-established role as a nexus for integrating cognitive, affective, and sensory information through its dense connections with both cortical and subcortical structures [31]. The consistent disruption of ACC-orbitofrontal connectivity aligns with models proposing that consciousness requires intact fronto-limbic integration [42], while the inferior temporal cortex's involvement may reflect compromised sensory-perceptual integration pathways [43].

The differential patterns of hyper-connectivity between VS and MCS patients provide crucial insights into potential recovery mechanisms. While the hypo-connected triangular network appears as a common pathological substrate, the state-specific hyper-connectivity patterns suggest distinct compensatory processes. This dissociation supports the view that consciousness disorders exist along a continuum of network dysfunction rather than as discrete categories.

The clinical implications of these findings are twofold. First, the conserved triangular hypo-connectivity pattern may serve as a diagnostic biomarker for DoC, particularly useful for differentiating true consciousness impairment from locked-in syndromes or other conditions [41]. Second, the state-specific hyper-connectivity patterns could guide therapeutic interventions. The persistence of the triangular network disruption across both patient groups suggests it may represent a minimal neural requirement for conscious awareness, while the variable hyper-connectivity patterns could reflect individual differences in residual plasticity and recovery potential.

4.4. Sensitivity of network analysis levels

Our findings demonstrate that different scales of network analysis provide complementary insights into the neural correlates of consciousness impairment. While global network measures showed preserved architecture across groups – consistent with studies showing macroscopic network resilience after brain injury [44] – macro- and local-level analyses revealed critical disruptions in specific subnetworks. This aligns with emerging frameworks in clinical neuroscience where focal connectivity alterations may drive functional deficits despite intact global topology [45]. The preserved global organization observed here may reflect compensatory mechanisms maintaining basic information routing, while finer-scale analyses uncover the pathological signatures of impaired consciousness.

Network measures like our modified PC offer valuable but generalized perspectives on segregation–integration balance. While effectively identifying in our analysis shifts toward increased inter-network connectivity at the expense of intra-network cohesion, a pattern observed in other neurological conditions [46], these metrics cannot fully capture the complex rewiring dynamics between subnetworks. Our PC variant proved particularly sensitive to group differences by synthesizing information about both the internal structure of LSNs and their external interactions.

Local-level connectivity analysis, though rich in detail, presents interpretational challenges when considered in isolation. The myriad of altered connections identified by NBS [13], while statistically robust, requires integration with macro-level findings to reveal their systemic implications. This limitation echoes debates in network neuroscience about reconciling micro-scale connectivity changes with their macro-scale functional consequences [47]. Our tripartite hypo-connectivity pattern (ACC-orbitofrontal-temporal) exemplifies how local disruptions gain meaning when contextualized within broader network architecture.

The multigraph approach addresses these limitations by unifying insights across scales. By combining PC data with intra- and inter-network connectivity alterations, our models reveal how local disruptions influence the entire system. This multiscale integration supports recent theoretical work emphasizing hierarchical network dysfunction in consciousness disorders [36].

4.5. Interpretation of multigraph model results

Our multigraph analysis reveals fundamental insights into how DoC disrupt the balance between integrative and segregative processes in LSNs. The significant differences in participation coefficients (green macronodes in Fig. 5) highlight specific LSNs where this balance is disturbed in patients, while the accompanying significant connection patterns elucidate the underlying network mechanisms. The directional patterns (HC > VS/MCS and VS/MCS > HC) reflect distinct hypoactive and hyperactive subnetworks, whose asymmetric organization suggests different compensatory strategies across patient groups.

A striking finding is the divergent reorganization between VS and MCS patients. VS patients exhibit more extensive hyperactivation patterns, potentially reflecting robust but maladaptive compensation. For instance, the normal PerN-SN pathway appears replaced by longer alternative routes (PerN-VAN-SN and PerN-Context-SN), suggesting inefficient network rerouting. In contrast, MCS patients show predominant hypoactivation with limited compensatory hyperactivation, particularly involving the ventral

attention network (VAN). This pattern implies partial functional restoration, where the VAN may partially assume perceptual functions normally mediated by the hypoactive PerN—a phenomenon supported by the rerouting of PerN-associated connections to VAN hub in MCS patients.

The perception network (PerN) emerges as a pivotal hub across conditions, underscoring its central role in conscious processing. Its consistent involvement, particularly the intra-network disconnection specific to MCS patients, aligns with evidence implicating sensory integration deficits in consciousness impairment [43]. The salience (SN) and context networks dominate VS reorganization, while VAN-centered changes characterize MCS, suggesting state-dependent vulnerability gradients. These patterns resonate with recent work showing hierarchical network dysfunction in consciousness disorders [36].

The most prominent disruptions occur in inter-network connectivity. VS patients show widespread SN hyperconnectivity (to VAN, cingulate operculum, context network, and default mode network), whereas MCS patients exhibit more targeted VAN-thalamocortical alterations. This dissociation suggests that while VS represents a state of global network dysregulation, MCS may reflect partial reintegration with residual VAN-mediated attention processes. The striatum's consistent involvement across states highlights its underappreciated role in network coordination during impaired consciousness.

These findings advance several key concepts. First, they identify a vulnerable “core axis” (VAN-SN-PerN-striatum) whose disruption may represent a minimal neural requirement for conscious awareness. Second, they demonstrate that compensation mechanisms differ qualitatively between VS and MCS—where VS shows extensive but inefficient rerouting, MCS exhibits more focused VAN-mediated reorganization. Third, the PerN's selective intra-network disruption in MCS.

The multigraph approach bridges an important gap between local connectivity changes and their system-wide consequences, demonstrating how multiscale network modeling can unravel the complexity of consciousness disorders. Clinically, this approach provides a powerful framework for differential diagnosis. The distinct hyper-hypoactivation signatures between VS and MCS offer objective markers of consciousness state, while the identified hub vulnerabilities suggest precise targets for neuromodulation. The systems-level perspective emphasizes that therapeutic strategies should address both hypoactive “core” networks and maladaptive hyperconnectivity patterns.

4.6. Neurophysiological implications

Our study revealed a distinct imbalance between integrative and segregative processes within large-scale brain networks in patients with DoC, ranging from VS to MCS, following anoxic brain injury. We identified characteristic patterns of both hyper- and hyposynchronized networks that differentially marked each clinical state. As demonstrated in Fig. 5 (multigraph model), the hypersynchronized subnetwork exhibited significantly greater spatial extent in VS patients compared to MCS cases.

Synchronization of neuronal activity in different brain structures is considered as a fundamental mechanism of information integration and formation of conscious perception. The coordinated activity of neuronal ensembles provides: unification of disparate sensory signals into a holistic subjective experience; global dissemination of information across distributed neuronal networks of the brain. Disruptions in this synchronized activity show strong correlations with DoC, including vegetative state/unresponsive wakefulness syndrome (VS/UWS) and minimally conscious state (MCS). This association underscores the critical role of large-scale neuronal synchronization in sustaining conscious awareness and higher-order cognitive processing.

We assume that the observed phenomenon in the VS group is related to the processes of compensation of the lost direct connections. Thus, in the norm (contrast $HC > VS$) there is a direct connection between the perception network and the salience network PerN-SN, which is compensated in the vegetative state (contrast $VS > HC$) by switching to the ventral attention network and the context network: PerN-VAN-SN and PerN-Context-SN. The PerN-Striatum connection is compensated again by switching to the PerN-Context-Striatum context network. The SN is well-established as a critical hub for processing information, including proprioceptive integration and maintaining wakefulness [48]. The engagement of the SN in perceptual processing under normal conditions, contrasted with its relative disconnection from perception networks in patients lacking signs of consciousness, supports the Global Workspace Theory [39,49]. This theory posits that consciousness functions as an integrative mechanism, overcoming functional segregation of brain structures and orchestrating their coordinated activity [50]. It should be emphasized that we cannot definitively state the purpose (nor the efficacy) of this compensatory mechanism. We can only hypothesize that this may represent the brain's attempt to restore environmental analysis capacity. This interpretation would align with Global Workspace Theory framework, wherein competing cognitive modules temporarily gain priority and constitute the contents of consciousness.

Regarding our findings on striatum involvement, current evidence suggests that without striatal input, the thalamus enters an inhibited state. As demonstrated by Schiff [40], this mechanism may play a pivotal role in the dysfunctional processes observed in DoC. This part of our data provides support for the mesocircuit model, which emphasizes the critical role of central thalamic neurons and their frontostriatal connections in maintaining consciousness [40]. This model proposes that recovery of forebrain mesocircuit function is closely linked to activation of the frontoparietal network, integrated within a “mesocircuit-frontoparietal” framework to explain the graded restoration of behavioral responsiveness across DoC severity levels [51–53]. Our finding of a shift to ventral attention network connectivity (PerN-SN) aligns with this framework. Notably, we observed selective engagement of the ventral frontoparietal subsystem—a network canonically associated with detecting unattended/unexpected stimuli and triggering attentional reorientation [54].

The contextual processing network – comprising the parahippocampal cortex, retrosplenial cortex, and medial prefrontal cortex – plays a fundamental role in evaluating the contextual significance of perceived stimuli [55]. However, the substantial anatomical and functional overlap between this network and the DMN [56] makes it challenging to attribute our observed compensatory switching

mechanism specifically to contextual processing. Notably, growing evidence suggests the DMN may be critically involved in this phenomenon, consistent with its established role in consciousness recovery across multiple studies [57–61].

In patients with MCS, we observed no significant hypersynchronization of the SN compared to healthy controls. This finding aligns with the results of Demertzi et al. [62], who demonstrated more pronounced SN impairment in VS/UWS patients relative to MCS cases.

Our data reveal the perception network (PerN) as the most critical hub, present in nearly all subnetworks. These results align with existing research demonstrating that reliance on phylogenetically older, low-organized networks achieves relatively high accuracy in discriminating consciousness levels [62,63].

In addition, our findings suggest that the hypoactive PerN-associated subnetwork in MCS patients may be functionally compensated by hyperactive VAN-centered circuitry. This implies that the VAN – functioning as the brain’s “radar” or stimulus-driven reorienting system [37,54,64] – potentially upregulates its activity, possibly enhancing sensitivity to diminished sensory input in MCS patients.

Our investigation has (1) pinpointed the neural architecture underlying this pathological state, and (2) identified compensatory mediator regions that restore functional connectivity balance. These findings transcend singular theoretical frameworks, instead validating aspects of both the Global Workspace Theory and Mesocircuit Model in chronic disorders of consciousness.

4.7. Complexity and nonlinearity in brain function

The brain’s functional architecture is characterized by nonlinear interactions, where small perturbations can lead to disproportionately large effects—a hallmark of chaotic systems [65]. This non-linearity is evident in our results, where local disruptions propagate to macro-scale network imbalances. Such dynamics challenge deterministic models of brain function, as they underscore the stochastic nature of state transitions [66,67]. This suggests that transitions between conscious states may follow random or nearly random processes. This is similar to the iso-energetic brain hypothesis, which states that minimal energy barriers facilitate rapid and unpredictable shifts in network configurations [67].

Our findings resonate with the Global Workspace Theory [39,49], where consciousness emerges from dynamic integration across distributed networks, and the Mesocircuit Model [40], which emphasizes thalamocortical interactions. The nonlinear loss of integration–segregation balance in DoC supports the idea that consciousness is a critical transition point in a high-dimensional parameter space [3]. However, the stochasticity of recovery trajectories cautions against over-reliance on deterministic biomarkers, highlighting the need for probabilistic models in clinical prognosis [67].

4.8. Limitations and future directions

A key limitation of our study is the absence of statistically significant differences when directly comparing VS and MCS patient groups across all analytical levels. This null finding likely stems from two interrelated factors: the modest sample sizes inherent to studies of severe brain injury populations, and the substantial heterogeneity within patient groups arising from diverse injury characteristics, durations, and recovery trajectories. Such variability is well-documented in DoC research, where individual differences in structural damage and functional reorganization often outweigh group-level patterns in small cohorts. Importantly, our inability to detect direct between-group differences does not necessarily indicate biological equivalence, but rather highlights the methodological challenges of comparing complex, multidimensional network alterations across heterogeneous patient populations.

While traditional statistical comparisons between patient groups proved underpowered, our multigraph modeling approach provided valuable qualitative insights into differential network mechanisms. The indirect comparison of VS and MCS multigraphs revealed distinct reorganization patterns. These observations align with emerging theoretical frameworks that view consciousness disorders as dynamic states along a recovery continuum rather than discrete categories. The qualitative differences in network topology suggest that direct patient group comparisons might require substantially larger samples to achieve statistical significance, given the multidimensional nature of network alterations and individual variability in compensatory processes.

Several methodological considerations should guide future research. First, larger multicenter cohorts could help overcome current sample size limitations while capturing the full spectrum of clinical heterogeneity. Second, longitudinal designs tracking network changes during recovery could clarify whether the observed patterns represent stable pathological signatures or transitional states. Third, incorporating multimodal data (e.g., structural connectivity, metabolomics) might help explain individual variability in functional network reorganization.

These limitations notwithstanding, our findings lay important groundwork for understanding hierarchical network dysfunction in anoxic DoC. The demonstrated approach of combining rigorous statistical testing with qualitative, model-based comparisons offers a template for studying complex neurological conditions where traditional group comparisons may obscure biologically meaningful patterns. Future studies building on this foundation could yield clinically actionable biomarkers for differential diagnosis and personalized treatment strategies.

Another limitation of the study is the specificity of the group. Anoxic brain injury represents only a small (and relatively understudied) etiological subgroup within the cohort of DoC patients, where the primary causes of this functional deficit remain traumatic brain injury (TBI) and, to a lesser extent, stroke. Despite the shared neurological symptom – reduced consciousness – it is currently challenging to extrapolate the obtained findings with absolute certainty to the entire cohort of patients.

Conclusions

Our multiscale network analysis provides a comprehensive framework for understanding the neural basis of disorders of consciousness following anoxic brain injury, revealing hierarchical disruptions that span global, macro-, and local levels of brain organization. While global network architecture remains preserved, reflecting structural resilience after injury, finer-scale analyses uncover critical disturbances in specific subnetworks – particularly in the ventral attention, salience, and perception networks – that underlie functional impairments. The opposing patterns of hypo- and hyperconnectivity observed in vegetative (VS) and minimally conscious (MCS) states suggest distinct pathophysiological mechanisms, with VS characterized by maladaptive compensatory hyperconnectivity and MCS by partial, VAN-mediated functional reorganization.

The clinical implications of these findings are twofold. First, the identified network signatures – such as the conserved triangular hypo-connectivity pattern (ACC-orbitofrontal-temporal) and state-specific hyperconnectivity profiles – offer objective biomarkers for differential diagnosis and prognosis. Second, the vulnerability of specific subnetworks, particularly the perception network, highlights promising targets for therapeutic interventions, including neuromodulation and personalized rehabilitation strategies. Our results advocate for a multiscale diagnostic approach that combines global screening with focused assessment of vulnerable subsystems to better capture the complexity of consciousness impairments.

These insights also advance theoretical understanding of consciousness as an emergent property of integrated network dynamics. The consistent involvement of a “core axis” (VAN-SN-PerN-striatum) supports models emphasizing the interplay between attention, sensory integration, and subcortical modulation in sustaining awareness. The multigraph approach, by bridging local- and macro-scale disruptions, provides a powerful tool for future research exploring network plasticity during recovery.

Future studies should address key unanswered questions: (1) How do these network patterns vary across injury etiologies (e.g., traumatic vs. anoxic)? (2) Can longitudinal tracking of multiscale connectivity predict recovery trajectories? (3) Do targeted interventions normalize the observed imbalances in integration–segregation? By addressing these questions, we can move closer to precision medicine approaches for disorders of consciousness, ultimately improving outcomes for this vulnerable patient population.

This work not only elucidates the network mechanisms of impaired consciousness but also establishes a methodological blueprint for studying multiscale brain dysfunction in other neurological and psychiatric conditions.

CRediT authorship contribution statement

S.A. Kurkin: Writing – original draft, Visualization, Supervision, Software, Project administration, Methodology, Investigation, Conceptualization. **L.A. Mayorova:** Writing – original draft, Supervision, Resources, Project administration, Methodology, Investigation, Funding acquisition, Data curation, Conceptualization. **V.S. Khorev:** Writing – original draft, Visualization, Software, Project administration, Methodology, Investigation, Conceptualization. **E.N. Pitsik:** Writing – review & editing, Visualization, Software, Methodology, Investigation. **M.L. Radutnaya:** Writing – review & editing, Methodology, Investigation, Data curation. **E.L. Bondar:** Writing – review & editing, Methodology, Investigation, Data curation. **A.E. Hramov:** Writing – review & editing, Supervision, Resources, Project administration, Methodology, Investigation, Funding acquisition, Conceptualization.

Declaration of competing interest

The authors declare that they have no known competing financial interests or personal relationships that could have appeared to influence the work reported in this paper.

Acknowledgments

The research was funded by the Ministry of Science and Higher Education of the Russian Federation.

Appendix

See [Tables 7](#) and [8](#).

Data availability

The data that support the findings of this study are not openly available due to reasons of sensitivity and are available from the corresponding author upon reasonable request.

Table 7

Between-group differences in clustering coefficient at the macro level across predefined large-scale networks (LSNs) without Bonferroni correction. Comparisons shown for healthy controls (HC), vegetative state (VS), and minimally conscious state (MCS) groups.

LSN	u-value HC > VS	p-value	u-value HC > MCS	p-value	u-value MCS > VS	p-value
COper	-0,795	0,426	0,579	0,563	-1,000	0,317
Context	-1,005	0,315	0,000	1,000	-0,722	0,470
DMN	-1,005	0,315	-0,424	0,671	-0,389	0,697
DAN	-1,046	0,295	-0,424	0,671	-0,500	0,617
perN	-0,628	0,530	0,193	0,847	-0,778	0,437
Somatomotor	-0,460	0,645	0,656	0,512	-0,722	0,470
Striatum	-0,209	0,834	0,656	0,512	-0,667	0,505
Thalamus	-0,586	0,558	0,501	0,616	-0,945	0,345
VAN	-0,921	0,357	-0,347	0,728	-0,278	0,781
Visual	-0,167	0,867	1,582	0,114	-0,889	0,374
FPN	-0,586	0,558	0,000	1,000	-0,722	0,470
SN	-1,172	0,241	-0,656	0,512	-0,445	0,657

Table 8

Between-group differences in node strength at the macro level across predefined large-scale networks (LSNs) without Bonferroni correction. Comparisons shown for healthy controls (HC), vegetative state (VS), and minimally conscious state (MCS) groups.

LSN	u-value HC > VS	p-value	u-value HC > MCS	p-value	u-value MCS > VS	p-value
COper	-0,699	0,485	0,656	0,512	-0,945	0,345
Context	-1,291	0,197	-0,656	0,512	-0,556	0,578
DMN	-1,164	0,244	-0,733	0,464	-0,056	0,956
DAN	-0,910	0,363	-0,270	0,787	-0,611	0,541
perN	-0,318	0,751	0,424	0,671	-0,889	0,374
Somatomotor	-0,487	0,626	0,656	0,512	-0,667	0,505
Striatum	0,318	0,751	0,964	0,335	-0,389	0,697
Thalamus	-0,656	0,512	0,579	0,563	-1,000	0,317
VAN	-1,122	0,262	-1,196	0,232	-0,167	0,868
Visual	0,275	0,783	1,736	0,083	-0,611	0,541
FPN	-0,953	0,341	0,000	1,000	-0,778	0,437
SN	-1,080	0,280	-0,733	0,464	-0,333	0,739

References

- [1] Li Ang, Liu Haiyang, Lei Xu, He Yini, Wu Qian, Yan Yan, Zhou Xin, Tian Xiaohan, Peng Yingjie, Huang Shangzheng, et al. Hierarchical fluctuation shapes a dynamic flow linked to states of consciousness. *Nat Commun* 2023;14(1):3238.
- [2] Blumenfeld Hal. Brain mechanisms of conscious awareness: detect, pulse, switch, and wave. *Neurosci* 2023;29(1):9–18.
- [3] Consortium Cogitate, Ferrante Oscar, Gorska-Klimowska Urszula, Henin Simon, Hirschhorn Rony, Khalaf Aya, Lepauvre Alex, Liu Ling, Richter David, Vidal Yamil, et al. Adversarial testing of global neuronal workspace and integrated information theories of consciousness. *Nat* 2025;1–10.
- [4] Luppi Andrea I, Craig Michael M, Pappas Ioannis, Finoia Paola, Williams Guy B, Allanson Judith, Pickard John D, Owen Adrian M, Naci Lorina, Menon David K, et al. Consciousness-specific dynamic interactions of brain integration and functional diversity. *Nat Commun* 2019;10(1):4616.
- [5] Papo David, Buldú Javier M, Boccaletti Stefano, Bullmore Edward T. Complex network theory and the brain. 2014.
- [6] Khorev Vladimir S, Kurkin Semen A, Zlateva Gabriella, Paunova Rositsa, Kandilarova Sevdalina, Maes Michael, Stoyanov Drozdostoy, Hramov Alexander E. Disruptions in segregation mechanisms in fMRI-based brain functional network predict the major depressive disorder condition. *Chaos Solitons Fractals* 2024;188:115566.
- [7] Hramov Aleksandr Evgen'evich, Frolov Nikita Sergeevich, Maksimenko Vladimir Aleksandrovich, Kurkin Semen Andreevich, Kazantsev Viktor Borisovich, Pisarchik Aleksandr N. Functional networks of the brain: from connectivity restoration to dynamic integration. *Phys-Usp* 2021;64(6):584.
- [8] Martín-Signes Mar, Chica Ana B, Bartolomeo Paolo, Thiebaut de Schotten Michel. Streams of conscious visual experience. *Commun Biol* 2024;7(1):908.
- [9] Schirmer Michael, Deco Gustavo, Ritter Petra. Learning how network structure shapes decision-making for bio-inspired computing. *Nat Commun* 2023;14(1):2963.
- [10] Fischer Michael, Rüegg Stephan, Czaplinski Adam, Strohmeier Monika, Lehmann Angelika, Tschan Franziska, Hunziker Patrick R, Marsch Stephan C. Inter-rater reliability of the full outline of UnResponsiveness score and the glasgow coma scale in critically ill patients: a prospective observational study. *Crit Care* 2010;14:1–9.
- [11] Giacino Joseph T, Kalmar Kathleen, Whyte John. The JFK coma recovery scale-revised: measurement characteristics and diagnostic utility. *Arch Phys Med Rehabil* 2004;85(12):2020–9.
- [12] SPM. SPM12. 2024, <http://www.fil.ion.ucl.ac.uk/spm/>. [Accessed 12 April 2024].
- [13] Khorev Vladimir, Kurkin Semen, Pitsik Elena, Radutnaya Margarita, Bondar Ekaterina, Mayorova Larisa, Hramov Alexander. A synergistic approach for identifying disrupted functional brain subnetworks in patients with chronic disorders of consciousness due to anoxic brain damage. *Eur Phys J Spec Top* 2025;1–12. <http://dx.doi.org/10.1140/epjs/s11734-024-01454-2>.
- [14] Kurkin Semen A, Smirnov Nikita M, Paunova Rositsa, Kandilarova Sevdalina, Stoyanov Drozdostoy, Mayorova Larisa, Hramov Alexander E. Beyond pairwise interactions: Higher-order Q-analysis of fMRI-based brain functional networks in patients with major depressive disorder. *IEEE Access* 2024;12:197168–86. <http://dx.doi.org/10.1109/ACCESS.2024.3521249>.
- [15] Andreev Andrey V, Kurkin Semen A, Stoyanov Drozdostoy, Badarin Artem A, Paunova Rossitsa, Hramov Alexander E. Toward interpretability of machine learning methods for the classification of patients with major depressive disorder based on functional network measures. *Chaos: An Interdiscip J Nonlinear Sci* 2023;33(6).

- [16] Rolls Edmund T, Huang Chu-Chung, Lin Ching-Po, Feng Jianfeng, Joliot Marc. Automated anatomical labelling atlas 3. *Neuroimage* 2020;206:116189.
- [17] Pitsik Elena N, Maximenko Vladimir A, Kurkin Semen A, Sergeev Alexander P, Stoyanov Drozdostoy, Paunova Rositsa, Kandilarova Sevdalina, Simeonova Denitsa, Hramov Alexander E. The topology of fMRI-based networks defines the performance of a graph neural network for the classification of patients with major depressive disorder. *Chaos Solitons Fractals* 2023;167:113041.
- [18] Pisarchik Alexander N, Andreev Andrey V, Kurkin Semen A, Stoyanov Drozdostoy, Badarin Artem A, Paunova Rossitsa, Hramov Alexander E. Topology switching during window thresholding fMRI-based functional networks of patients with major depressive disorder: Consensus network approach. *Chaos: An Interdiscip J Nonlinear Sci* 2023;33(9).
- [19] Yang Shi-Qi, Xu Zhi-Peng, Xiong Ying, Zhan Ya-Feng, Guo Lin-Ying, Zhang Shun, Jiang Ri-Feng, Yao Yi-Hao, Qin Yuan-Yuan, Wang Jian-Zhi, et al. Altered intranetwork and internetwork functional connectivity in type 2 diabetes mellitus with and without cognitive impairment. *Sci Rep* 2016;6(1):32980.
- [20] Wang Chunli, Cai Huanhuan, Sun Xuettian, Si Li, Zhang Min, Xu Yuanhong, Qian Yinfeng, Zhu Jiajia. Large-scale internetwork functional connectivity mediates the relationship between serum triglyceride and working memory in young adulthood. *Neural Plast* 2020;2020(1):8894868.
- [21] Kelly Clare, Castellanos F Xavier. Strengthening connections: functional connectivity and brain plasticity. *Neuropsychol Rev* 2014;24:63–76.
- [22] Hardikar Samyogita, McKeown Brontë, Schaare H Lina, Wallace Raven Star, Xu Ting, Lauckner Mark Edgar, Valk Sofie Louise, Margulies Daniel S, Turnbull Adam, Bernhardt Boris C, et al. Macro-scale patterns in functional connectivity associated with ongoing thought patterns and dispositional traits. *Elife* 2024;13:RP93689.
- [23] Zwir Igor, Arnedo Javier, Mesa Alberto, Del Val Coral, de Erausquin Gabriel A, Cloninger C Robert. Temperament & character account for brain functional connectivity at rest: A diathesis-stress model of functional dysregulation in psychosis. *Mol Psychiatry* 2023;28(6):2238–53.
- [24] Boccaletti Stefano, Latora Vito, Moreno Yamir, Chavez Martin, Hwang D-U. Complex networks: Structure and dynamics. *Phys Rep* 2006;424(4–5):175–308.
- [25] Costantini Giulio, Perugini Marco. Generalization of clustering coefficients to signed correlation networks. *PloS One* 2014;9(2):e88669.
- [26] Rubinov Mikail, Sporns Olaf. Weight-conserving characterization of complex functional brain networks. *Neuroimage* 2011;56(4):2068–79.
- [27] Onnela Jukka-Pekka, Saramäki Jari, Kertész János, Kaski Kimmo. Intensity and coherence of motifs in weighted complex networks. *Phys Rev E—Stat Nonlinear Soft Matter Phys* 2005;71(6):065103.
- [28] Newman Mark EJ. The mathematics of networks. *New Palgrave Encycl Econ* 2008;2(2008):1–12.
- [29] Guimera Roger, Nunes Amaral Luís A. Functional cartography of complex metabolic networks. *Nat* 2005;433(7028):895–900.
- [30] Zalesky Andrew, Fornito Alex, Bullmore Edward T. Network-based statistic: identifying differences in brain networks. *Neuroimage* 2010;53(4):1197–207.
- [31] Seeley William W, Menon Vinod, Schatzberg Alan F, Keller Jennifer, Glover Gary H, Kenna Heather, Reiss Allan L, Greicius Michael D. Dissociable intrinsic connectivity networks for salience processing and executive control. *J Neurosci* 2007;27(9):2349–56.
- [32] Goulden Nia, Khusnulnisa Ayyul, Davis Nicholas J, Bracewell Robert M, Bokde Arun L, McNulty Jonathan P, Mullins Paul G. The salience network is responsible for switching between the default mode network and the central executive network: replication from DCM. *Neuroimage* 2014;99:180–90.
- [33] Chang Catie, Glover Gary H. Time–frequency dynamics of resting-state brain connectivity measured with fMRI. *Neuroimage* 2010;50(1):81–98.
- [34] Boly Melanie, Garrido Marta Isabel, Gosseries Olivia, Bruno Marie-Aurélië, Boveroux Pierre, Schnakers Caroline, Massimini Marcello, Litvak Vladimir, Laureys Steven, Friston Karl. Preserved feedforward but impaired top-down processes in the vegetative state. *Sci* 2011;332(6031):858–62.
- [35] Laureys Steven, Owen Adrian M, Schiff Nicholas D. Brain function in coma, vegetative state, and related disorders. *Lancet Neurol* 2004;3(9):537–46.
- [36] Demertzi Athena, Tagliazucchi Enzo, Dehaene Stanislas, Deco Gustavo, Barttfeld Pablo, Raimondo Federico, Martial Charlotte, Fernández-Espejo Davinia, Rohaut Benjamin, Voss HU, et al. Human consciousness is supported by dynamic complex patterns of brain signal coordination. *Sci Adv* 2019;5(2):eaat7603.
- [37] Corbetta Maurizio, Patel Gaurav, Shulman Gordon L. The reorienting system of the human brain: from environment to theory of mind. *Neuron* 2008;58(3):306–24.
- [38] Tononi Giulio, Boly Melanie, Massimini Marcello, Koch Christof. Integrated information theory: from consciousness to its physical substrate. *Nature Rev Neurosci* 2016;17(7):450–61.
- [39] Dehaene Stanislas, Changeux Jean-Pierre, Naccache Lionel. The global neuronal workspace model of conscious access: from neuronal architectures to clinical applications. In: *Characterizing consciousness: From cognition to the clinic?* Springer; 2011, p. 55–84.
- [40] Schiff Nicholas D. Recovery of consciousness after brain injury: a mesocircuit hypothesis. *Trends Neurosci* 2010;33(1):1–9.
- [41] Edlow Brian L, Claassen Jan, Schiff Nicholas D, Greer David M. Recovery from disorders of consciousness: mechanisms, prognosis and emerging therapies. *Nat Rev Neurol* 2021;17(3):135–56.
- [42] Laureys Steven, Gosseries Olivia, Tononi Giulio. In: *The neurology of consciousness: cognitive neuroscience and neuropathology*, Academic Press; 2015.
- [43] Boly Melanie, Massimini Marcello, Tsuchiya Naotsugu, Postle Bradley R, Koch Christof, Tononi Giulio. Are the neural correlates of consciousness in the front or in the back of the cerebral cortex? Clinical and neuroimaging evidence. *J Neurosci* 2017;37(40):9603–13.
- [44] Kim Eunhyung, Seo Han Gil, Seong Min Yong, Kang Min-Gu, Kim Heejae, Lee Min Yong, Yoo Roh-Eul, Hwang Inpyeong, Choi Seung Hong, Oh Byung-Mo. An exploratory study on functional connectivity after mild traumatic brain injury: Preserved global but altered local organization. *Brain Behav* 2022;12(9):e2735.
- [45] Fornito Alex, Zalesky Andrew, Breakspear Michael. The connectomics of brain disorders. *Nature Rev Neurosci* 2015;16(3):159–72.
- [46] Gratton Caterina, Nomura Emi M, Pérez Fernando, D'Esposito Mark. Focal brain lesions to critical locations cause widespread disruption of the modular organization of the brain. *J Cogn Neurosci* 2012;24(6):1275–85.
- [47] Park Hae-Jeong, Friston Karl. Structural and functional brain networks: from connections to cognition. *Sci* 2013;342(6158):1238411.
- [48] Craig Arthur D. How do you feel—now? The anterior insula and human awareness. *Nature Rev Neurosci* 2009;10(1):59–70.
- [49] Baars Bernard J. The global workspace theory of consciousness: Predictions and results. In: *The Blackwell companion to consciousness*. Wiley Online Library; 2017, p. 227–42.
- [50] Baars Bernard J. The conscious access hypothesis: origins and recent evidence. *Trends Cogn Sci* 2002;6(1):47–52.
- [51] Laureys Steven, Schiff Nicholas D. Coma and consciousness: paradigms (re) framed by neuroimaging. *Neuroimage* 2012;61(2):478–91.
- [52] Vanhaudenhuyse Audrey, Noirhomme Quentin, Tshibanda Luaba J-F, Bruno Marie-Aurélië, Boveroux Pierre, Schnakers Caroline, Soddu Andrea, Perlberg Vincent, Ledoux Didier, Brichant Jean-François, et al. Default network connectivity reflects the level of consciousness in non-communicative brain-damaged patients. *Brain* 2010;133(1):161–71.
- [53] Wu Xuehai, Zou Qihong, Hu Jin, Tang Weijun, Mao Ying, Gao Liang, Zhu Jianhong, Jin Yi, Wu Xin, Lu Lu, et al. Intrinsic functional connectivity patterns predict consciousness level and recovery outcome in acquired brain injury. *J Neurosci* 2015;35(37):12932–46.
- [54] Corbetta Maurizio, Shulman Gordon L. Control of goal-directed and stimulus-driven attention in the brain. *Nature Rev Neurosci* 2002;3(3):201–15.
- [55] Kveraga Kestutis, Ghuman Avniel Singh, Kassam Karim S, Aminoff Elissa A, Hämäläinen Matti S, Chaumon Maximilien, Bar Moshe. Early onset of neural synchronization in the contextual associations network. *Proc Natl Acad Sci* 2011;108(8):3389–94.
- [56] Bar Moshe, Aminoff Elissa, Mason Malia, Fenske Mark. The units of thought. *Hippocampus* 2007;17(6):420–8.
- [57] Coulborn Sean, Taylor Chris, Naci Lorina, Owen Adrian M, Fernández-Espejo Davinia. Disruptions in effective connectivity within and between default mode network and anterior forebrain mesocircuit in prolonged disorders of consciousness. *Brain Sci* 2021;11(6):749.
- [58] Crone Julia S, Lutkenhoff Evan S, Vespa Paul M, Monti Martin M. A systematic investigation of the association between network dynamics in the human brain and the state of consciousness. *Neurosci Conscious* 2020;2020(1):niaa008.
- [59] Fernández-Espejo Davinia, Soddu Andrea, Cruse Damian, Palacios Eva M, Junque Carme, Vanhaudenhuyse Audrey, Rivas Eva, Newcombe Virginia, Menon David K, Pickard John D, et al. A role for the default mode network in the bases of disorders of consciousness. *Ann Neurol* 2012;72(3):335–43.

- [60] Hannawi Yousef, Lindquist Martin A, Caffo Brian S, Sair Haris I, Stevens Robert D. Resting brain activity in disorders of consciousness: a systematic review and meta-analysis. *Neurol* 2015;84(12):1272–80.
- [61] Norton Loretta, Hutchison RM, Young G Bryan, Lee Donald H, Sharpe Michael D, Mirsattari SM. Disruptions of functional connectivity in the default mode network of comatose patients. *Neurol* 2012;78(3):175–81.
- [62] Demertzi Athena, Antonopoulos Georgios, Heine Lizette, Voss Henning U, Crone Julia Sophia, de Los Angeles Carlo, Bahri Mohamed Ali, Di Perri Carol, Vanhaudenhuyse Audrey, Charland-Verville Vanessa, et al. Intrinsic functional connectivity differentiates minimally conscious from unresponsive patients. *Brain* 2015;138(9):2619–31.
- [63] Medina Jean Paul, Nigri Anna, Stanziano Mario, D'Incerti Ludovico, Sattin Davide, Ferraro Stefania, Rossi Sebastiano Davide, Pinardi Chiara, Marotta Giorgio, Leonardi Matilde, et al. Resting-state fMRI in chronic patients with disorders of consciousness: the role of lower-order networks for clinical assessment. *Brain Sci* 2022;12(3):355.
- [64] Vossel Simone, Geng Joy J, Fink Gereon R. Dorsal and ventral attention systems: distinct neural circuits but collaborative roles. *Neurosci* 2014;20(2):150–9.
- [65] Golberger AL. Non-linear dynamics for clinicians: chaos theory, fractals, and complexity at the bedside. *Lancet* 1996;347(9011):1312–4.
- [66] Korf Jakob, Gramsbergen Jan Bert. Timing of potential and metabolic brain energy. *J Neurochem* 2007;103(5):1697–708.
- [67] Stojanov Drozdostoy, Korf Jakob, De Jonge Peter, Popov Georgi. The possibility of evidence-based psychiatry: depression as a case. *Clin Epigenetics* 2011;2(1):7–15.